16.2 FURTHER EVALUATION OF AN URBAN CANOPY PARAMETERIZATION USING VTMX AND URBAN 2000 DATA

Hung-Neng S. Chin and Martin J. Leach

Lawrence Livermore National Laboratory, Livermore, California

1. INTRODUCTION

Almost two-thirds of the U.S. population live in urbanized areas occupying less than 2% of the landmass. Similar statistics of urbanization exists in other parts of the world. With the rapid growth of the world population, urbanization appears to be an important issue on environmental and health aspects. As a result, the interaction between the urban region and atmospheric processes becomes a very complex problem. Further understanding of this interaction via the surface and/or atmosphere is of importance to improve the weather forecast, and to minimize the loss caused by the weather-related events, or even by the chemical-biological threat.

To this end, Brown and Willaims, (1998) first developed an urban canopy scheme to parameterize the urban infrastructure effect. This parameterization accounts for the effects of drag, turbulent production, radiation balance, and anthropogenic and rooftop heating. Further modification was made and tested in our recent sensitivity study for an idealized case using a mesoscale model. Results indicated that the addition of the rooftop surface energy equation enables this parameterization to more realistically simulate the urban infrastructure impact (Chin et al., 2000).

To further improve the representation of the urban effect in the mesoscale model, the USGS land-use data with different resolutions (200 and 30 meters) are adopted to derive the urban parameters via a look-up table approach (Leone et al., 2002; Chin et al., 2004). This approach can provide us the key parameters for urban infrastructure and urban surface characteristics to drive the urban canopy parameterization with geographic and temporal dependence. These urban characteristics include urban fraction, roof fraction, building height, anthropogenic heating, surface albedo, surface wetness, and surface roughness.

The objective of this study is to evaluate the modified urban canopy parameterization (UCP) with the observed measurements. Another objective is to demonstrate the deficiency of using limited numbers of single-station meteorological measurements to validate the urban impact in the mesoscale models. The final objective of this study is to assess the value of tracer data in assessing the performance of UCP.

2. MODEL AND INITIAL CONDITIONS

The Naval Research Laboratory's 3-D coupled Ocean/Atmosphere mesoscale prediction system (COAMPS) is used to study the urban impacts on low-level atmospheric momentum and heat transport, and surface energy budget. COAMPS consists of a data assimilation system, a nonhydrostatic atmospheric forecast model, and a hydrostatic ocean model. However, to minimize the impact of the data assimilation on the performance of UCP, all the simulations shown are conducted using the cold-start approach.

In this study, we use only the atmospheric forecast model, which is composed of a compressible form of the dynamics, nest-grid capability, and parameterizations of subgrid-scale mixing, surface momentum and heat fluxes, explicit ice microphysics, subgrid-scale cumulus clouds, and shortwave and longwave radiation. The terrain-following vertical coordinate is also used to simulate flow over an irregular surface. The reader is referred to Hodur (1997) for further details of COAMPS. Description of the modified UCP can be seen in Chin et al. (2000 and 2004).

The model domain contains 35 grid points in the vertical, with the grid size varied to maximize resolution at lower levels. The grid spacing of the lowest layer is 4 m, with each successive layer aloft smoothly increased. The domain top resides at the altitude of 35.898 km. In the horizontal, both coordinates have 61 grid points for all nest grid domains. A uniform grid size of 36 km is used for the outer coarse mesh. A constant grid size ratio of three is applied to define the inner nest grids. A total of four nests are performed in this study.

Constant time steps of 90 and 45 seconds for non-sound and sound wave calculations, respectively, are used in the coarser grids for the time-splitting scheme. The time steps for the finer-grid domains are reduced proportionally to the nest-grid size ratios. The rigid boundary condition is imposed at the vertical boundary. A sponge-damping layer is placed above 12.8 km to minimize the reflection of internal gravity waves off the rigid upper boundary. The Davies (1976) boundary condition is applied to the lateral boundaries with a nudging zone of seven grid points at each lateral boundary. A time filter with a coefficient of 0.2 is applied to control computational instability associated with the leapfrog time approximation in the model.

The initial and lateral boundary conditions of simulations are based on the ETA data with a horizontal resolution of 40 km from the National Centers for Environmental Prediction. The intensive observational period (IOP) occurring on 25-26 October (IOP-10) during VTMX 2000 is selected for this study as a representative of high wind environment. Based on surface station measurements, the urban heat island (UHI) index of this case (~ 3 °C) falls into the lower end of the UHI spectrum (few to 12 °C) reviewed by Oke (1973 and 1982). This weak UHI index is consistent with the inverse correlation of UHI with the ambient wind speed reported by Hildebrand and Ackerman (1984), and Morris and Simmonds (2001).

* *Corresponding author address*: Dr. Chin, Lawrence Livermore National Lab. (L-103), Livermore, CA 94550; e-mail: chin2@llnl.gov.

UCRL-CONF-204547

Due to the inherent limitation of single-station measurements on validating the urban impact in the mesoscale models, tracer concentration data of SF_6 are also utilized as supplemental observations to evaluate the performance of UCP in the mesoscale model. To this end, COAMPS forecast is used as inputs to a dispersion model for the calculation of the tracer concentration during the tracer release time. This tracer calculation is conducted using Lawrence Livermore National Laboratory's Lagrangian Operational Dispersion Integrator (LODI). The details of this dispersion model can be seen in Ermak and Nasstrom (2000). To assess the overall performance of UCP in a variety of urban conditions, the validation for all IOPs with tracer releases (i.e., IOP-2, 4, 5, 7 for low wind and line source, and IOP-9, and 10 for high wind and point source) are also performed in this study.

3. Experiment Design

In this research, we conduct a series of sensitivity experiments with the finest horizontal resolution of 1.33 km using ETA 40-km data. First, simulations with and without the urban effect are performed to gauge the urban influence on the mesoscale processes. Second, simulations with the urban parameters from different resolutions of land-use data (200 and 30 meters, respectively) are used to evaluate the sensitivity of urban parameters to the modeled urban effect. Third, the experiments with varied nest grids (i.e., 3 and 4 nests) are conducted to study the impact of horizontal resolution (4 km and 1.33 km, respectively) on the urban canopy parameterization. Last, sensitivity experiments are also performed to quantitatively gauge the relative contribution of anthropogenic heating, urban infrastructure and urban surface to the overall urban effect on the mesoscale processes.

4. RESULTS

The urban impact on the model prediction is assessed by comparing model simulations with derived urban forcing using different resolutions of USGS land-use data (referred to as UCP_30m and UCP_200m, respectively) and with the simulation without the urban forcing (no_UCP).

The evolutions of vertical profiles of predicted temperature at the COAMPS grid point nearest station M04 from the simulations with and without the urban effect are displayed in Figure 1. This station is selected by the fact that the largest urban thermal forcing from the rooftop and anthropogenic heating within the fourth-nest domain is located near this grid point. Without the urban impact, the no_UCP simulation shows a clear nighttime low-level inversion layer over the entire model domain (Fig. 1a). With the urban canopy scheme turned on, the temperature inversion becomes weakened in the urban area. However, the inversion layer structure still exists in most of the model domain, except for some locations near station M04. For the simulations with the urban forcing, an elevated inversion layer starts to appear above a neutral surface layer at 26 hours of UCP simulations (i.e., one hour after the sunrise), and lasts for only two hours. The delay and the short persistence time of the elevated inversion layer in this case is due in great part to the weaker urban nocturnal heating, which is involved in a complicated interaction among urban infrastructure, local topography and strong ambient wind. The lingering of nocturnal heat island effect can also impact other types of scale interaction. Yoshikado (1992) reported an analog situation for the delay of sea breeze progression.

In this study, the top of the modeled urban canopy at station M04 resides at 9 and 18 meters above the ground for the 30-m and 200-m resolutions of land-use data, respectively. However the temperature response of the urban canopy reaches higher altitudes due to the enhanced turbulence production and its transport of heat (Fig. 2). The depth of the predicted urban boundary layer (22 and 36 meters for UCP_30m and UCP_200m, respectively) is nearly twice the urban canopy height in the simulations with the urban impact for this weak heat island case. A similar finding was reported in an earlier field study (Uno et al. 1988).

The impact of UCP on the horizontal wind field at the station M04 is depicted in Figure 3. A clear diurnal cycle of valley winds is identified in both no_UCP and UCP simulations (Fig. 3a). The predicted low-level nocturnal jet at 27 hours of the no_UCP simulation is elevated by approximately 20 meters in the UCP_200m run. This elevated jet-like wind profile is in response to the enhanced low-level TKE from the combined urban heat island (buoyancy) and urban drag (mechanic) effects. As a result, the vertical transport of momentum by turbulence modifies the horizontal velocity field by slowing down the near-surface air and accelerating the layer aloft. This urban impact is stronger in the 200-m run than in the 30-m simulation due to the larger urban forcing in the 200-m land-use data (Figs. 3b and 3c). In addition, a noticeable wind direction shift of approximately 20° clockwise is identified in the predicted afternoon wind profile with the UCP (e.g., at 33 hours of simulation time) while a weaker wind shift of 10° or so counter-clockwise is seen in the nighttime. A similar urban wind shift effect has been reported in earlier field studies (Angell et al. 1971; Draxler 1986).

In most of the simulations described in this paper, the COAMPS model resolution was prescribed as 1.33km. To test the effects at coarser resolution, a simulation with horizontal resolution of 4km was also executed. Results indicate that the coarser resolution leads to weaker urban forcing, which produces weaker turbulence (Figs. 4b and 2c). As a result, a well-defined nocturnal urban boundary layer with elevated inversion aloft does not form in the coarser resolution simulation although the surface inversion layer is substantially weakened (Figs. 4a and 1c). Similar results also appear in the UCP_200m simulations (not shown).

The effects of anthropogenic heating, urban surface properties and urban infrastructure characteristics were also tested in this study. The effects of no anthropogenic heating appear to be minimal (Fig. 5a and 1b). This is not a surprising result, as the amount of anthropogenic heating that was prescribed is small (< 30 W m^{-2}). In addition, when the urban surface properties are not defined in the parameterization, a nocturnal urban boundary layer still develops in response to the urban infrastructure parameters alone (Fig. 5b). Finally, when including urban surface properties but excluding the infrastructure effects, no elevated inversion layer forms and the urban effects are minimal (Fig. 5c).

According to these sensitivity studies, the combined effects of street canyons and building rooftops have the most pronounced influence on the urban boundary layer properties. Further sensitivity studies indicate that the street canyon effect is much weaker than the rooftop effect in this urban canopy parameterization (not shown). Therefore, the rooftop effect is the dominant contributor to the thermal field in the urban boundary layer. This result is similar to UHI observations (Oke 1995).

To validate the urban impact on the mesoscale model, COAMPS simulations are evaluated using standard meteorological measurements and the SF_6 tracer data. The root-mean-square errors (RMSE) of the predicted near-surface wind direction and speed, and temperature for IOP-10 are presented in Figure 6. Using the results at every forecast hour from the model simulations over the entire simulation period of 36 hours, these RMSE are calculated with respect to the data obtained from Utah meso-net, VTMX 2000, and Urban 2000 stations. The stations chosen are ordered such that lower station numbers correspond to smaller amounts of roof fraction, i.e. urbanization increases in the positive x-direction. Note that the larger differences than 90 degrees of wind direction between simulations and observations are on purpose removed from the RMSE calculations. This adjustment acts to minimize the impact of bad forecast or uncertain measurements particularly in the situation with near calm wind. As a whole, the number of removed samples is pretty small at each station while they can substantially increase RMSE and contaminate the signal on detecting the wind shift by the urban effect.

It is clear from the wind direction trace (Fig. 6a) that higher RMSEs appear at the stations with larger roof fraction. The difference of RMSEs between non-urban and urban runs tends to be small at the stations with lower roof fractions while this magnitude increases in the areas with larger urban impact. Although the UCP has an effect to reduce the RMSE of wind direction, the magnitude is still much smaller than the total RMSE. This suggests that the single-station observations are not representative of the area equivalent to the mesoscale grid size. However, further observational evidence and modeling studies are necessary to substantiate this conclusion.

In contrast to the wind-direction trace, the wind-speed RMSE does not exhibit the clear dependence on urbanization (Fig. 6b). However, the RMSE is reduced with increasing urbanization as a result of increased urban drag in the simulations with the urban canopy parameterization. On the other hand, temperature forecasts show resemblance of close dependence on urbanization, i.e. increased RMSE in the areas with larger roof fraction (Fig. 6c). In addition, simulations with the urban effect seem to result in larger temperature RMSEs at the urban grids than their non-urban counterparts. This outcome is consistent with the stronger nighttime urban warming and weaker daytime cooling in the simulations with small anthropogenic heating. Therefore, net urban warming is expected in the RMSE calculations.

These RMSE calculations clearly demonstrate the limitations of using single-station data in urban areas to evaluate the performance of UCP on the wind and temperature forecasts in the mesoscale model. However, SF_6 tracer data collected during the URBAN 2000 experiment can be used for this purpose. Data collected at any individual sampler is the result of the integration of the wind vectors as the tracer travels from the source to the sampler. Individual building or urban surface effects are therefore averaged along the trajectory. The wind field predictions, along with stability indices, from COAMPS simulations are used to drive the Lagrangian particle dispersion model (LODI) to create predicted SF_6 concentrations. The observed hourly-integrated tracer surface concentrations from 100 NOAA samplers are interpolated onto a 9 km x 9 km grid domain that has been defined for the LODI simulations.

Using the tracer data for validation, simulations of IOP-10 with the UCP substantially improve the plume forecasts (Fig. 7). The predicted plume using the UCP forecast for both resolutions of land-use data shifts 20-30 degrees to the right, and is consistent with the wind shift seen in the wind direction predictions at earlier morning hours. This urban effect on plume prediction and wind direction forecast is consistent with the finding of earlier studies (Angell et al., 1971; Draxler, 1986). The better agreement with tracer concentration data using the UCP also supports the wind speed forecast, as concentration transports away from the source more quickly without the UCP. As a whole, there are trivial differences in the plume forecasts using different resolutions of land-use data sets.

Further validation of tracer data for a variety of urban conditions in URBAN 2000 is also shown in Fig. 8. Results indicate that the plume forecasts are persistently improved in all six IOPs with tracer releases in URBAN 2000 when the UCP is used. The only exception occurs in IOP-5 after 2 hours of release time. Generally speaking, the modified UCP noticeably improves the plume forecasts in a variety of urban conditions. This outcome supports the improvement of wind forecast with UCP in the mesoscale model.

5. SUMMARY AND DISCUSSION

In this paper, we present a modified version of BW's urban canopy scheme (1998) by adding the rooftop surface energy equation and additional changes to more realistically simulate the urban impact in the mesoscale model. Measurements from the field experiments of VTMX 2000 and URBAN 2000 are used to assess the urban impact on surface and near-surface atmospheric properties using NRL's three-dimensional mesoscale model, COAMPS. Both conventional surface station measurements and tracer concentration observations are utilized to gauge the performance of UCP for the sub-grid building effect in the mesoscale model.

A series of sensitivity experiments are performed to gain our understanding of the urban impact on the mesoscale aspects of atmospheric properties for a case with strong scale interaction over an area with the complex terrain. The contribution of urban morphology and model grid resolution to the formation of elevated inversion layer and its associated urban boundary layer is also addressed in this research.

Results indicate that under the urban environment with clear-sky and strong drainage flow over the Salt Lake Valley, urban surface characteristics and anthropogenic heating plays little role in the formation of

the nocturnal urban boundary layer. This outcome agrees with an earlier remark on the effect of anthropogenic heating on the genesis of UHI in most cities (Oke 1995). The main contributor to this urban boundary layer is attributed to the building rooftop effect. Sensitivity test also shows that the model horizontal grid resolution is important in simulating the elevated inversion layer for this weak UHI case.

The results using derived urban properties from different resolutions of USGS land-use data indicate that the 200-m date set leads to a stronger urban forcing than the 30-m case as a result of more urban landmass categories considered in the coarser resolution of land-use data. Nonetheless, the higher resolution of land-use data has a better improvement on the surface properties of local lake water. Sensitivity experiments further reveals that the depth of the predicted urban boundary layer is about twice the urban canopy height in this weak UHI case, and that this ratio is nearly constant despite the type of land-use data. The same ratio was reported in an earlier field study (Uno et al., 1988). However, a higher ratio of three to four was also observed in the cities of the metropolitan size (Bornstein 1968).

The root mean square errors of predicted wind and temperature with respect to the surface station measurements exhibit fairly large discrepancies at the urban locations. However, the close agreement of modeled tracer concentration with observations fairly justifies the modeled urban impact on the wind direction shift and wind drag effects. This result further confirms the finding of an earlier observational study regarding the inappropriate representative of single-station measurements to the urban environment (Draxler 1986). Generally speaking, our results indicate that the consideration of both thermal and mechanic aspects of sub-grid building effects in the urban canopy parameterization is of importance to predict a better wind forecast in the urban areas.

As shown earlier, the use of single-station measurements for the validation of the mesoscale model can cause substantial bias to the model forecast. However, this bias may be reduced by the measurements from multiple stations, which can represent different portions of the surrounding urban environment. Thus, the weighting average of multiple-station measurements may have more value to verify the urban impact in the mesoscale model. The consideration of this problem in the future field studies would be very helpful for the improvement of urban modeling work. Finally, the fair agreement of tracer data in the UCP validation for six case studies in URBAN 2000, representing a variety of urban conditions, provides a strong support for this modified urban canopy scheme to simulate the urban impact in the mesoscale model.

Acknowledgments. The authors wish to thank NRL for providing us the COAMPS model to test the urban canopy parameterization in the mesoscale model. We also thank DOE Environmental Meteorology, and Chemical and Biological National Security Programs for using VTMX 2000 and URBAN 2000 data to validate the model results. This work was supported by the Department of Energy Chemical-Biological National Security Program and conducted under the auspices of the U.S. Department of Energy by the University of California, Lawrence Livermore National Laboratory under Contract W-7405-Eng-48.

6. REFERENCES

Angell, J. K., D. H. Pack, C. R. Dickson, and W. H. Hoecker, 1971: Urban influence on nighttime airflow estimated from Tetroon flights. *J. Appli. Meteorol.*, **10**, 194-204.

Bornstein, R. A., 1968: Observations of the urban heat island effects in New York City. *J. Appl. Meteor.*, **7**, 575-582.

Brown, M. J. and M. Willams, 1998: An Urban Canopy Parameterization for Mesoscale Meteorological Models. *Proceedings of the AMS Conference on 2nd Urban Environment Symposium*, 2-7 November, 1998, Albuquerque, New Mexico, Amer. Meteor. Soc., 144-147.

Chin, H.-N. S., M. J. Leach, and M. J. Brown, 2000: A preliminary study of the urban canopy effects on a regional-scale model: Sensitivity assessment of an idealized case. *Proceedings of the third Symposium on the Urban Environment,* July 14-18, 2000, Davis, California, Amer. Meteor. Soc., 76-77.

Chin, H.-N. S., M. J. Leach, G. A. Sugiyama, J. M. Leone Jr., H. Walker, J. S. Nasstrom, and M. J. Brown, 2004: Evaluation of an urban canopy parameterization in a mesoscale model using VTMX and URBAN 2000 data. *Mon. Wea. Rev.* (Submitted)

Davies, H. C., 1976: A lateral boundary formulation for multi-level prediction models. *Quart. J. Roy. Meteor. Soc.,* **102**, 405-418.

Draxler, R. R., 1986: Simulated and observed influence of the nocturnal heat island on the local wind field. J. Climate and Appl. Meteorol. Soc., **25**, 1125-1133.

Ermak, D.L., and J.S. Nasstrom, 2000: A Lagrangian stochastic diffusion method for inhomogeneous turbulence, Atmos. Environ., **34**, 1059-1068.

Hildebrand, P. H., and B. Ackerman, 1984: Urban effects on the convective boundary layer. *J. Atmos. Sci.*, **41**, 76-91.

Hodur, R., 1997: The Naval Research Laboratory's coupled ocean-atmospheric mesoscale prediction system (COAMPS). *Mon. Wea. Rev.*, **125**, 1414-1430.

Morris, C. J. G., and I. Simmonds, 2001: Quantification of the influences of wind and cloud on the nocturnal urban heat island of a large city. *J. Appl. Meteor.*, **40**, 169-182.

Oke, T. R., 1973: City size and the urban heat island. *Atmos. Environ.*, **7**, 769-779.

Oke, T. R., 1982: The Energetic basis of the Urban heat island, *Quart. J. Royal Meteor. Soc.*, **108**, 1-24.

Oke, T. R., 1995: The heat island of the urban boundary layer: Characteristics, causes and effects. *Wind Climate in Cities*, J. E. Cermak et al., Eds., NATO ASI Series E, Vol. 227, Kluwer Academic, 81-107.

Uno, I., S. Wakamatsu, H. Ueda, and A. Nakamura, 1988: An observational study of the structure of the nocturnal urban boundary layer. *Bound.-Layer Meteor.*, **45**, 59-82.

Yoshikado, H., 1992: Numerical study of the daytime urban effect and its interaction with the sea breeze. *J. Appli. Meteorol.*, **31**, 1146-1164.

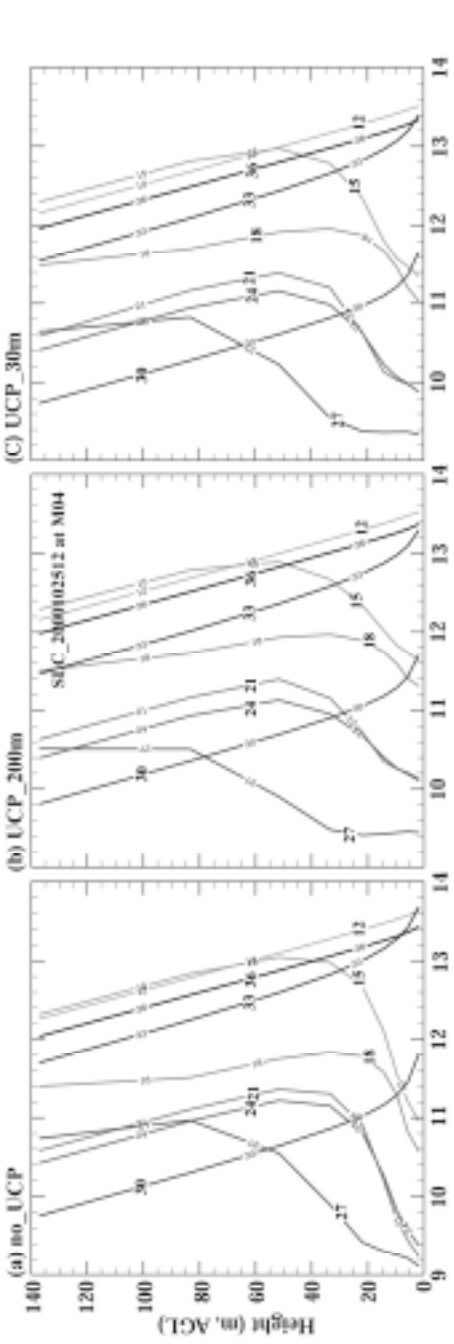

Fig. 1. Evolutions of the vertical profiles for the predicted temperature field at the model grid near the station M04. The curves on the plots are labeled by the forecast time of the simulation. (a) for the no_UCP run, (b) for the UCP_200m run, and (c) for the UCP_30m run.

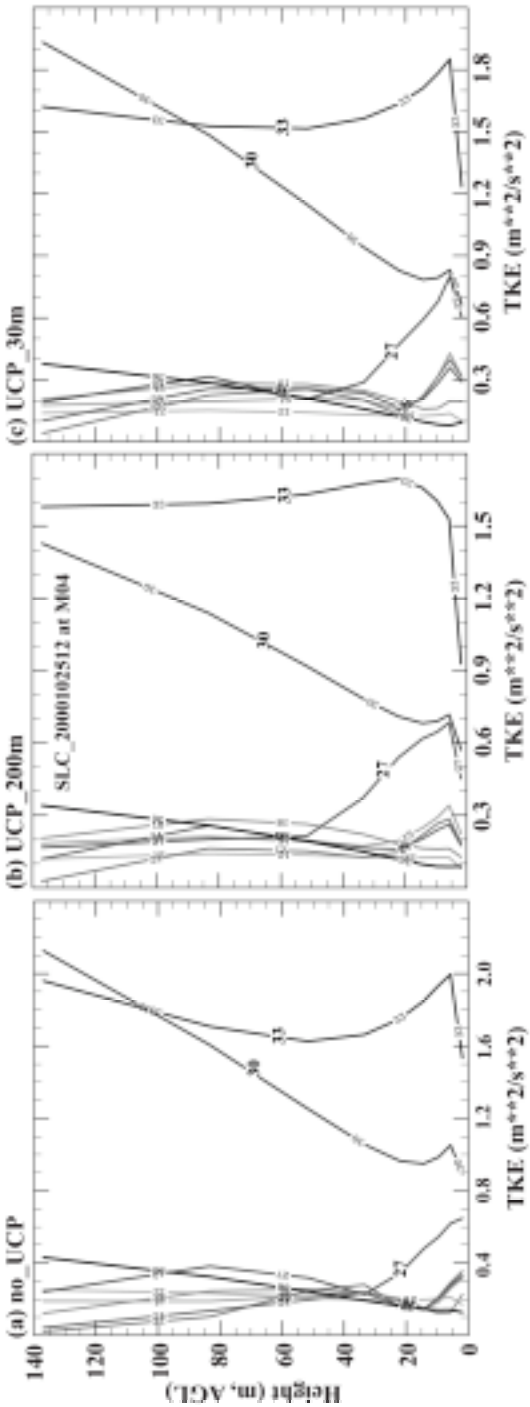

Fig. 2. As in Fig. 1, except for the turbulence kinetic energy field.

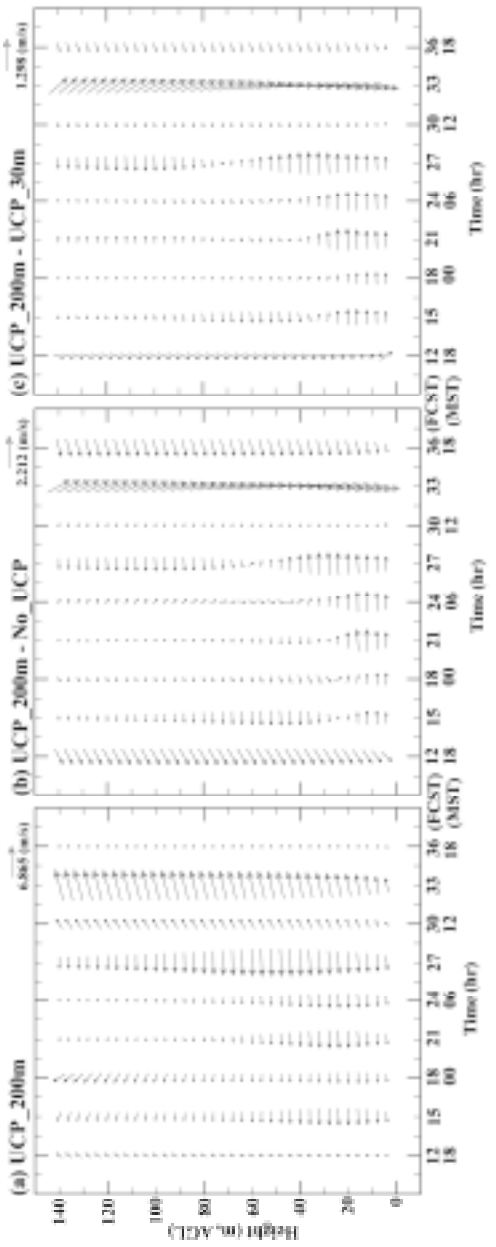

Fig. 3. Evolutions of the vertical profiles for the predicted horizontal winds at the model grid near the station M04. (a) for the UCP_200m run, (b) for the deviation between UCP_200m and no_UCP, (c) for the deviation between UCP_200m and UCP_30m.

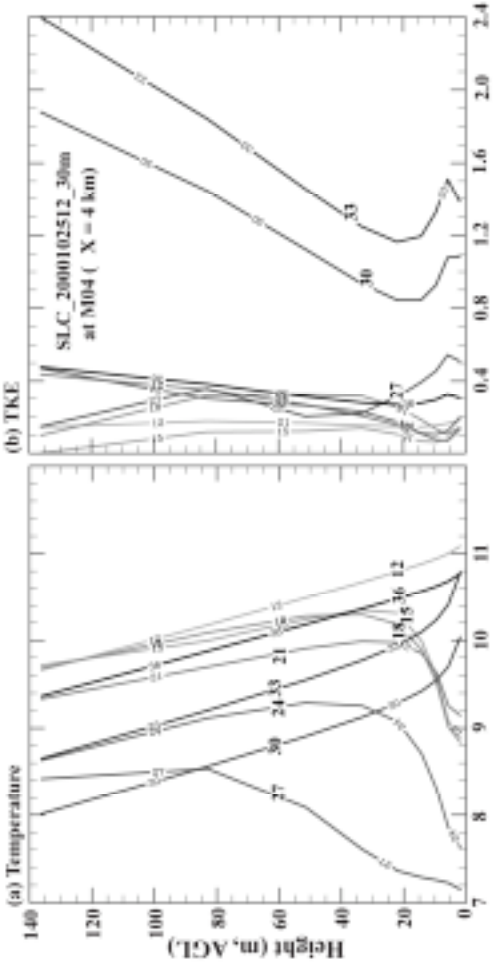

Fig. 4. As in Figs 1 and 2, except for the nest-3 of the UCP_30m run.

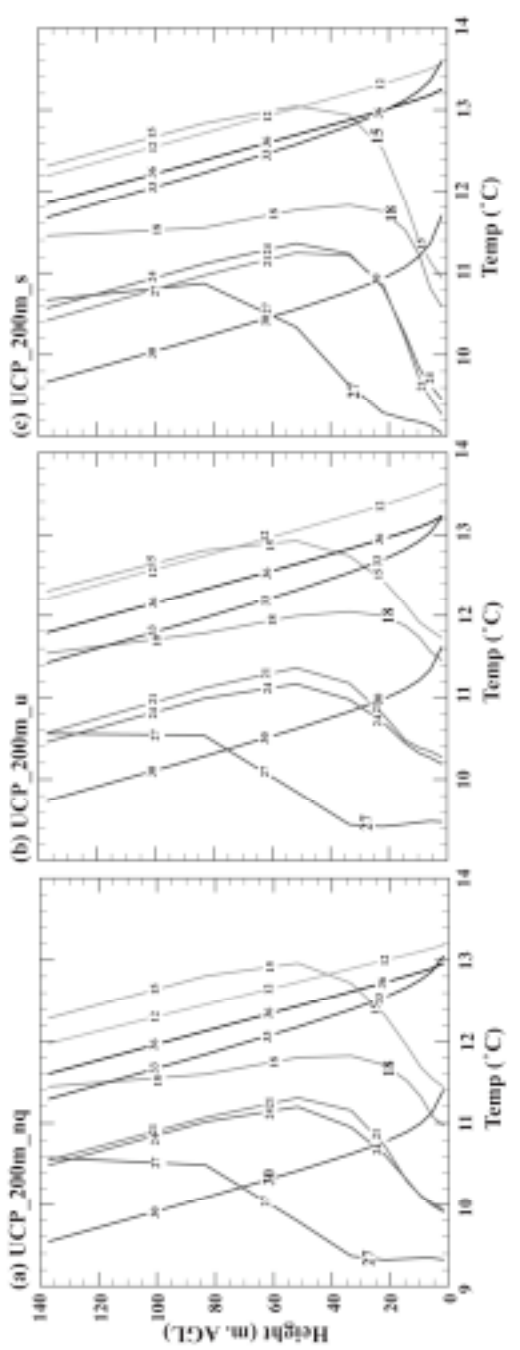

Fig. 5. As in Fig. 1, except for the UCP_200m runs. (a) no anthropogenic heating, (b) without using land-use data derived urban surface properties, (c) without using land-use data derived urban infrastructure properties.

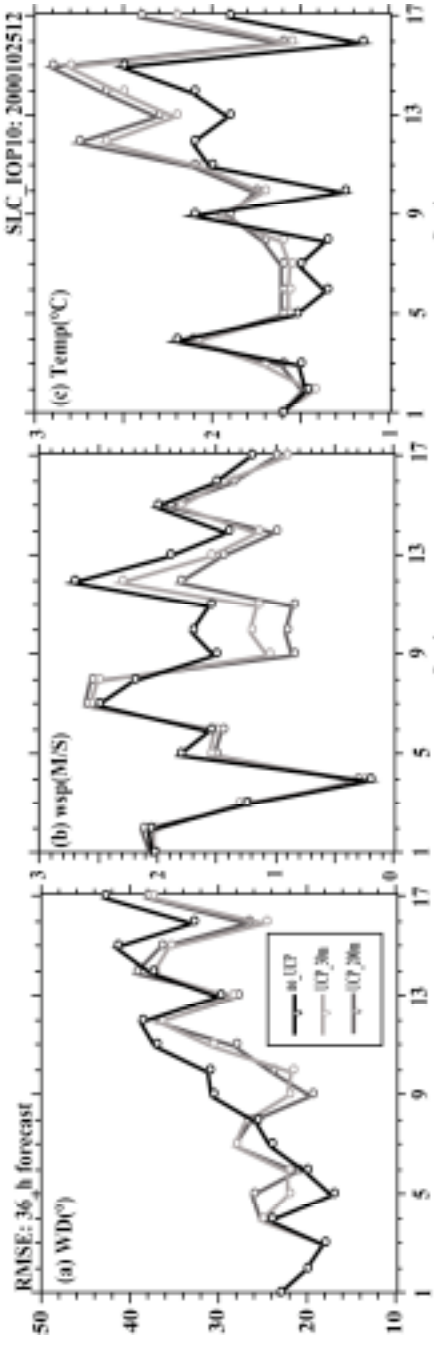

Fig. 6. Root mean square errors of 36-h forecasts with respect to the surface station measurements for the nest-4 to the surface station measurements for the nest-4 simulations with different configurations of urban measurements for the nest-4 simulations with different configurations of urban properties at selected stations.

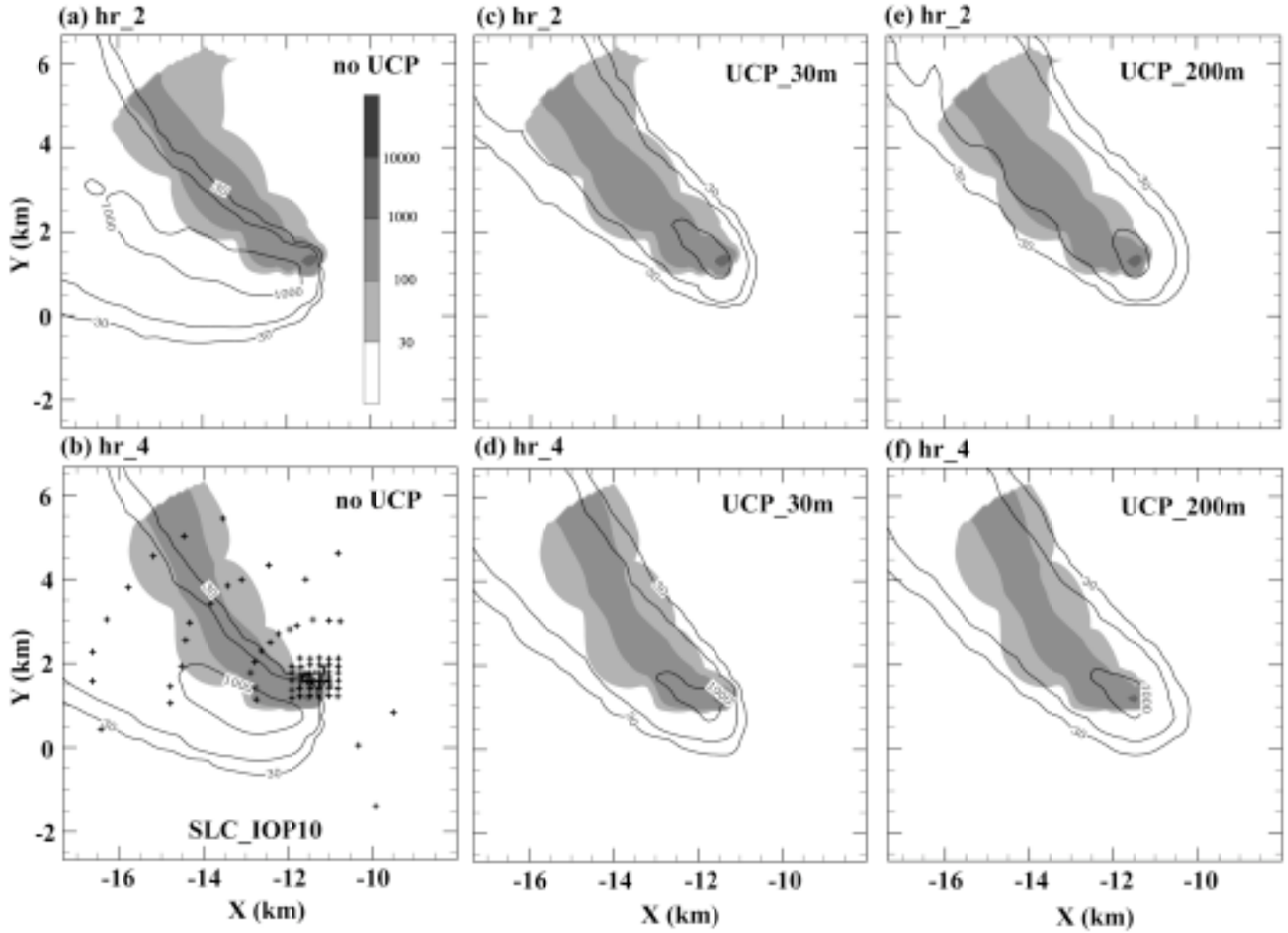

Fig. 7. Horizontal cross-sections of hourly-averaged modeled (contour) and observed (color bar) surface SF_6 concentrations in unit of parts per billion. The simulated concentrations are calculated using LLNL's Lagrangian Operational Dispersion Integrator based on COAMPS's prediction without and with the urban canopy parameterization for different resolutions of land-use data. The pictures are shown at the second and fourth hours from the tracer release time, which correspond to 21 and 23 hours of simulation time in the COAMPS forecast. The plus sign shown in (b) marks the locations of NOAA samplers with tracer data.

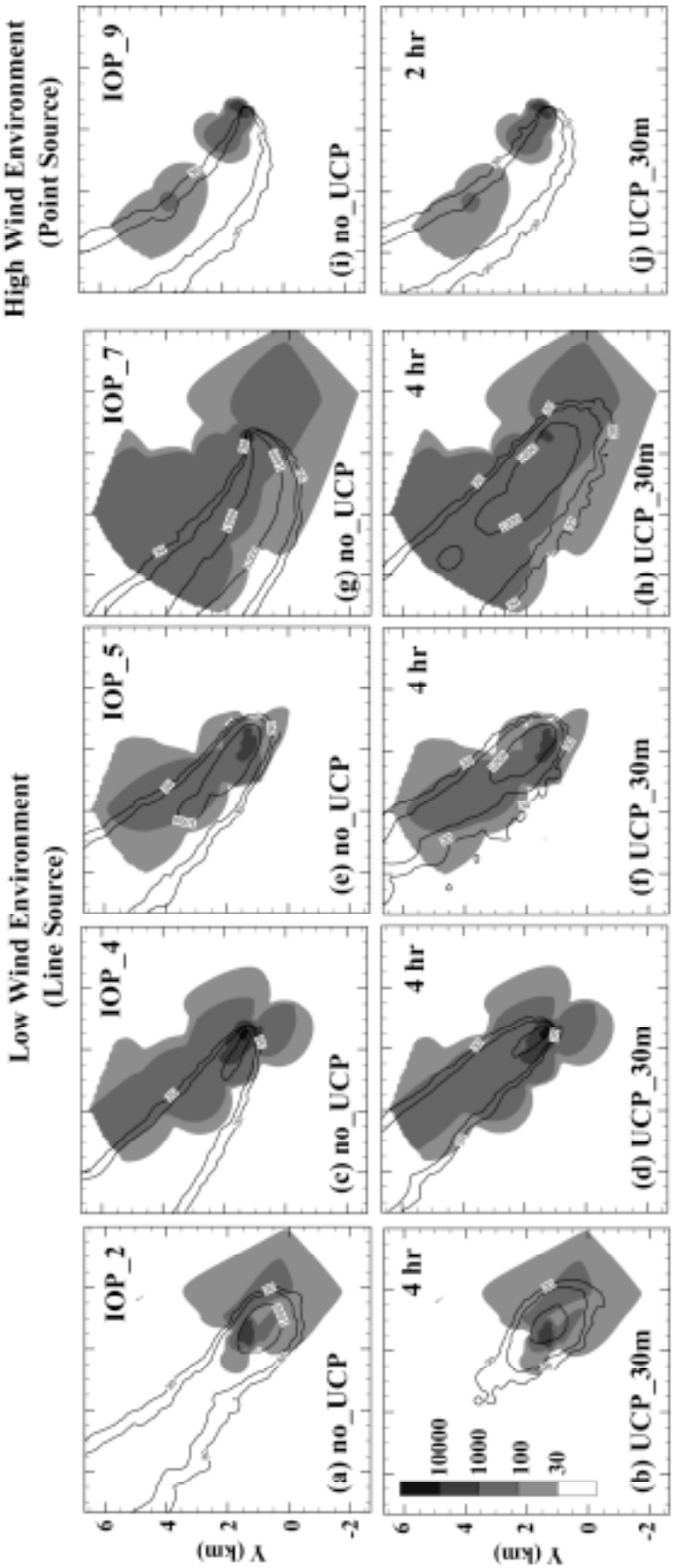

Fig. 8. As in Fig. 7, except for IOPs of 2, 4, 5 and 7 in the low wind environment, and for IOP-9 in the high wind environment. All SF6 concentrations are shown at hour 4 from the initial release time, except for IOP-9 at hour 2.